scientific reports

Check for updates

OPEN

Enhancing the economic feasibility of vaterite production using calcium hydroxide in pH-swing processes

Won Jo[1] & Myoung-Jin Kim[1,2,3]✉

The challenge of cost-effective and efficient indirect carbonation processes is significant. This study aimed to address the limitations associated with alkaline additives, which are among the primary factors negatively affecting the economic viability of the indirect carbonation process. Specifically, we evaluated the feasibility of replacing NaOH, a commonly used alkaline additive, with $Ca(OH)_2$, a more cost-effective and safer alternative. Particular emphasis was placed on the potential production of fine-particle vaterite $CaCO_3$, which, despite its high industrial applicability, poses production challenges owing to its inherent instability. Experiments were conducted to evaluate the impact of using $Ca(OH)_2$, with and without sucrose, on the production yield, morphology, particle size, and purity of $CaCO_3$, in comparison to NaOH. Despite the low solubility of $Ca(OH)_2$, its combination with sucrose effectively stabilized pH levels and significantly enhanced $CaCO_3$ yields. The addition of sucrose further increased supersaturation, aiding vaterite formation. Using $Ca(OH)_2$ with sucrose resulted in a vaterite content exceeding 95%, similar to that achieved with NaOH. A cost analysis revealed that producing vaterite-type $CaCO_3$ using $Ca(OH)_2$ combined with sucrose required only 53% of the cost associated with NaOH, demonstrating its superior economic feasibility. These findings establish $Ca(OH)_2$, particularly in combination with sucrose, as a viable alternative to NaOH in the pH swing process, providing cost savings, improved safety, and high-purity vaterite-type $CaCO_3$ suitable for various industrial applications.

Keywords Vaterite, Calcium hydroxide, pH-swing, Sucrose, Indirect carbonation, Alkaline agent

In 2023, global CO_2 emissions reached 37.4 billion tons, with atmospheric CO_2 concentrations averaging 419 ppm, increasing by approximately 2.5 ppm annually since 2010[1,2]. This increase has exacerbated climate change, leading to global warming, ocean acidification, extreme weather events, and sea-level rise, significantly damaging ecosystems and disrupting industrial and economic systems[3–5]. To address these challenges, carbon capture, utilization, and storage (CCUS) technologies, including indirect carbonation, offer promising solutions by converting CO_2 into $CaCO_3$ and $MgCO_3$[6–17]. Recent research has highlighted an emerging and promising trend toward using widely available industrial alkaline mineral wastes (steel slags[6–8,10], gypsum[12,13], and cement kiln dust (CKD)[14,15]) as sustainable calcium sources for $CaCO_3$ manufacturing. Utilizing these waste materials offers substantial sustainability benefits, reduces manufacturing costs, addresses environmental and safety concerns, and effectively supports CCUS objectives, significantly contributing towards circular economy goals.

The pH-swing process in carbonation involves the use of alkaline additives for two primary purposes: adjusting the pH to precipitate impurities as hydroxides, thereby enhancing carbonate purity and facilitating CO_3^{2-} formation to increase carbonate production [7,10–15,18–21]. This technique includes the extraction of calcium and magnesium at low pH levels, followed by their precipitation as carbonates at high pH levels, which effectively promotes high-purity carbonate production. Elevating the pH level is crucial for the efficient precipitation of carbonates and ensuring the quality of the final product. This method achieves high carbonation efficiency under mild, low-energy conditions at atmospheric pressure, offering an advantage over alternative approaches such as direct aqueous or gas–solid carbonation[21].

[1]Department of Convergence Study on the Ocean Science and Technology, Korea Maritime and Ocean University, Busan 49112, Korea. [2]Department of Environmental Engineering, Korea Maritime and Ocean University, Busan 49112, Korea. [3]Interdisciplinary Major of Ocean Renewable Energy Engineering, Korea Maritime and Ocean University, Busan 49112, Korea. ✉email: kimmj@kmou.ac.kr

The pH-swing process, while effective, has significant limitations owing to its high consumption of chemicals. This increased chemical usage inherently raises the overall cost of the process compared to alternative methods, potentially making it less cost-effective[21]. Furthermore, the inability to recover these chemicals poses a significant challenge for scaling up this technology to an industrial level. However, producing high-purity products plays a crucial role in mitigating these costs[7,10–15,18–22]. Another effective strategy for reducing overall expenses is the use of inexpensive or free indirect carbonation solvents[15,23–26]. Equally important is the identification of a cost-efficient and effective alkaline agent for the pH swing process.

Vaterite, despite being an unstable polymorph of calcium carbonate, is recognized as a highly promising industrial material due to its distinctive properties, including high specific surface area, solubility, porosity, and dispersibility. These characteristics make it particularly suitable for various applications in pharmaceuticals, cosmetics, and functional materials[23–25]. However, its inherent instability and sensitivity to synthesis conditions have historically presented substantial challenges to achieving large-scale production[24].

Sodium hydroxide and ammonium hydroxide, commonly used as alkali additives in the pH swing process, are relatively costly chemicals that may lack economic feasibility for large-scale processes requiring significant quantities. Additionally, their strong alkalinity and corrosive nature can result in equipment and reactor corrosion, as well as pose significant health risks, such as severe irritation to the skin, eyes, and respiratory system, necessitating cautious handling. Sodium hydroxide, also known as caustic soda, is a potent base and highly corrosive compound that readily dissolves in water, ionizing into Na^+ and OH^- ions, allowing it to rapidly elevate pH through the OH^- ions[27]. However, during operations, NaOH reacts with atmospheric CO_2, forming Na_2CO_3, which can compromise its purity. Similarly, owing to the high volatility of NH_4OH, maintaining precise pH control during operations is challenging [28]. Paradoxically, these alkali additives, designed to enhance process efficiency and product quality, can undermine the economic viability of processes and introduce additional operational complexities. To reduce overall process costs, inexpensive alkalis, such as $Ca(OH)_2$, can serve as effective substitutes for NaOH. $Ca(OH)_2$, commonly known as slaked lime, is a widely used and cost-effective alkali product[27]. Compared to NaOH, which costs $719/ton, $Ca(OH)_2$ is significantly more cost-effective at $227/ton and provides enhanced handling safety[29,30]. However, a notable drawback of $Ca(OH)_2$ is its low solubility in water (0.16 g $Ca(OH)_2$/100 g water at 20 °C)[31].

To date, $Ca(OH)_2$ has not been employed as an alkaline agent in the pH swing process for indirect carbonation, primarily due to its notably low solubility in water, as documented in previous studies[6–17] (Table S1). Moreover, no prior research has explored its application for producing vaterite-type $CaCO_3$ through this method. This study addresses that gap by evaluating the use of cost-effective $Ca(OH)_2$, combined with sucrose, as a viable alternative to the more expensive NaOH[32]. This approach not only enhances economic feasibility but also introduces an innovative dissolution–precipitation-induced mineralization mechanism, enabling both the recovery of calcium and the in-situ formation of high-purity vaterite-type $CaCO_3$.

This study aims to enhance the economic viability of alkali additives by replacing NaOH with $Ca(OH)_2$. The utilization of $Ca(OH)_2$ not only attains the required high pH levels for the procedure but also provides extra calcium during carbonation, thereby enhancing the production of vaterite-type $CaCO_3$. Furthermore, $Ca(OH)_2$ is notably more economical than NaOH and simpler to handle. This substitution enhances the advantages of alkali additives while mitigating their constraints.

To evaluate the feasibility of utilizing $Ca(OH)_2$ as a substitute for conventional alkali additives, experiments were conducted under uniform conditions, with the sole distinction being the alkali additive used, either $Ca(OH)_2$ or NaOH. The properties of the produced $CaCO_3$ were examined and juxtaposed in relation to its attributes, such as morphology, particle size, and cost-effectiveness.

Materials and methods

Materials and analytical instruments

The calcium source used in this study was cement kiln dust (CKD) from a cement manufacturing company in Saudi Arabia. Artificial desalination brine, prepared according to the procedure outlined by Kester et al. (1967)[33], was used as the solvent for calcium elution. NaOH (Sodium Hydroxide Pellet 97%, Duksan), $Ca(OH)_2$ (Calcium Hydroxide 95%, Duksan), and sucrose (White sugar, CJ CheilJedang) were added during the carbonation process in their original, unprocessed forms.

The CKD characteristics and the morphology and purity of the $CaCO_3$ produced via the carbonation process were examined using X-ray diffraction (XRD, SmartLab, Rigaku, Japan) and X-ray fluorescence spectrometry (XRF, XRF-1800, Shimadzu, Japan). XRD analysis was performed with CuK-α radiation at 40 kV/30 mA, with measurements conducted over a 2θ range of 10.0° to 70.0° at intervals of 0.04°. The calcite and vaterite contents were calculated based on the XRD results using Rao's equation[34]. The $CaCO_3$ purity was determined from the XRF results by analyzing the elemental composition, including calcium. The particle size of $CaCO_3$ was assessed using a laser scattering particle size analyzer (PSA, Mastersizer 3000, Malvern) with the wet method, employing distilled water as the dispersing medium. Before measurement, an ultrasonic disperser ensured proper dispersion of solid particles. The particle size was evaluated based on the D_{50} value, and the particle size distribution was also examined. The surface structure of $CaCO_3$ was analyzed using scanning electron microscopy (SEM, MIRA-3, Tescan, Czech Republic). For the SEM analysis, the solid samples were gold-coated and observed using a secondary electron (SE) detector at an accelerating voltage of 5.0 kV. The calcium concentration in the liquid samples from the experiments was quantified using an atomic absorption spectrometer (AAS, AA200, Perkin Elmer, USA).

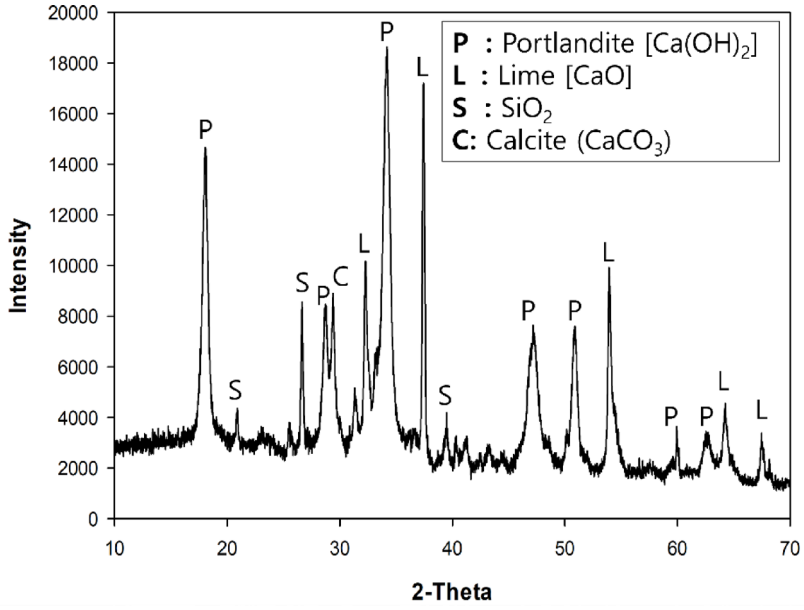

Fig. 1. XRD patterns of CKD.

Content	CaO	Al_2O_3	SiO_2	K_2O	Fe_2O_3	SO_3	MgO	Others
wt%	76.8	8.8	4.1	3.1	2.4	2.0	1.5	1.3

Table 1. XRF analysis results of CKD.

Methods

Calcium elution

Calcium elution was conducted by combining CKD and artificial brine at a ratio of 1:25 (g:mL) in a 3 L cylindrical reactor. The mixture was stirred at 200 rpm for 30 min, after which the resulting suspension was filtered through a 0.45 μm membrane filter to obtain the calcium eluate used in the subsequent carbonation experiments. The complete calcium elution procedure was conducted under ambient temperature and atmospheric pressure conditions.

Carbonation

The carbonation experiment involved adding $Ca(OH)_2$ and sucrose to 100 mL of calcium eluate, then introducing CO_2 at a flow rate of 0.15 L/min. The concentrations of $Ca(OH)_2$ were varied at 0, 25, 50, 100, 150, and 200 mM, while sucrose was added at concentrations of 0, 10, 25, 50, and 100 mM. The pH of the solution was continuously monitored during carbonation, and CO_2 injection ceased when the pH reached 7.5 to prevent $CaCO_3$ re-dissolution. Following carbonation, the suspension was filtered using a 0.45 μm membrane to isolate $CaCO_3$, which was subsequently dried at 70 °C for 24 h. $CaCO_3$ was characterized using techniques such as XRD, SEM, PSA, and XRF. The $CaCO_3$ production yield was determined by the difference in calcium concentration between the initial eluate and the filtrate post-carbonation. An additional experiment using NaOH instead of $Ca(OH)_2$ was conducted under the same conditions for comparison. A control experiment without alkali additives was also performed, and the results were compared with those of the alkali additive. All carbonation reactions were conducted at ambient temperature and atmospheric pressure.

Techno-economic analysis

Economic viability was evaluated by comparing total production costs for vaterite-type $CaCO_3$ synthesized using $Ca(OH)_2$ combined with sucrose against that using NaOH. The cost analysis was based on current market prices for $Ca(OH)_2$, sucrose, and NaOH, allowing for a quantitative evaluation of the potential cost savings achieved by substituting $Ca(OH)_2$ and sucrose for NaOH.

Results and discussion

Characterization of CKD and desalination brine

XRD analysis of CKD identified portlandite ($Ca(OH)_2$), lime (CaO), and calcite ($CaCO_3$) as the dominant phases, with a minor presence of SiO_2 (Fig. 1). XRF analysis indicated a high CaO content of 76.8%, alongside Al_2O_3, SiO_2, K_2O, and Fe_2O_3 at 8.8%, 4.1%, 3.1%, and 2.4% by weight, respectively (Table 1). The substantial calcium content in CKD, primarily in the forms of $Ca(OH)_2$ and CaO, which are readily soluble in brine, demonstrates its suitability as an industrial by-product for indirect carbonation. Additionally, the artificial desalination brine

exhibits concentrations of individual components approximately twice as high as those found in seawater, as outlined in Table S2.

Calcium elution

The calcium concentration in the eluate was 5415 ± 274 mg/L, with a pH of 12.3 ± 0.2. The process of calcium elution by brine is elucidated by the following reactions:

$$MgCl_2\,(aq) + CaO\,(s) + H_2O\,(l) \rightarrow Mg\,(OH)_2\,(s) + CaCl_2\,(aq) \quad (1)$$

$$MgCl_2\,(aq) + Ca\,(OH)_2\,(s) \rightarrow Mg\,(OH)_2\,(s) + CaCl_2\,(aq) \quad (2)$$

In these reactions, Mg in the brine precipitates as $Mg(OH)_2$, while Ca is eluted from CaO and $Ca(OH)_2$ present in CKD[35,36]. Furthermore, CaO and $Ca(OH)_2$ in CKD react with the high concentration of NaCl in the brine, resulting in Ca elution and a rise in pH[37]:

$$2NaCl\,(aq) + CaO\,(s) + H_2O\,(l) \rightarrow CaCl_2\,(aq) + 2NaOH\,(aq) \quad (3)$$

$$2NaCl\,(aq) + Ca\,(OH)_2\,(s) \rightarrow CaCl_2\,(aq) + 2NaOH\,(aq) \quad (4)$$

Carbonation

Changes in pH upon the addition of alkaline additives

Figure 2 illustrates the impact of various alkali agents on pH fluctuations during the carbonation process. The experiments were carried out under three conditions: a control with 50 mM sucrose, 100 mM $Ca(OH)_2$ with 50 mM sucrose, and 100 mM NaOH with 50 mM sucrose. Preliminary tests showed that sucrose promoted the dissolution of $Ca(OH)_2$. To ensure a fair comparison between the performance of $Ca(OH)_2$ and NaOH, 50 mM sucrose was included in both experimental setups. Throughout carbonation, the pH of the solution gradually decreased (Fig. 2). Alkaline additives like $Ca(OH)_2$ and NaOH notably boosted the pH buffering capacity on CO_2 dissolution compared to the control trial. This pH reduction is attributed to the subsequent reactions[38]:

$$CO_2\,(g) \leftrightarrow CO_2\,(aq) \quad (5)$$

$$CO_2\,(aq) + H_2O\,(l) \leftrightarrow H_2CO_3\,(aq) \quad (6)$$

$$H_2CO_3\,(aq) \leftrightarrow H^+\,(aq) + HCO_3^-\,(aq) \quad (7)$$

$$HCO_3^-\,(aq) \leftrightarrow H^+\,(aq) + CO_3^{2-}\,(aq) \quad (8)$$

$$Ca^{2+}\,(aq) + CO_3^{2-}\,(aq) \leftrightarrow CaCO_3\,(s) \quad (9)$$

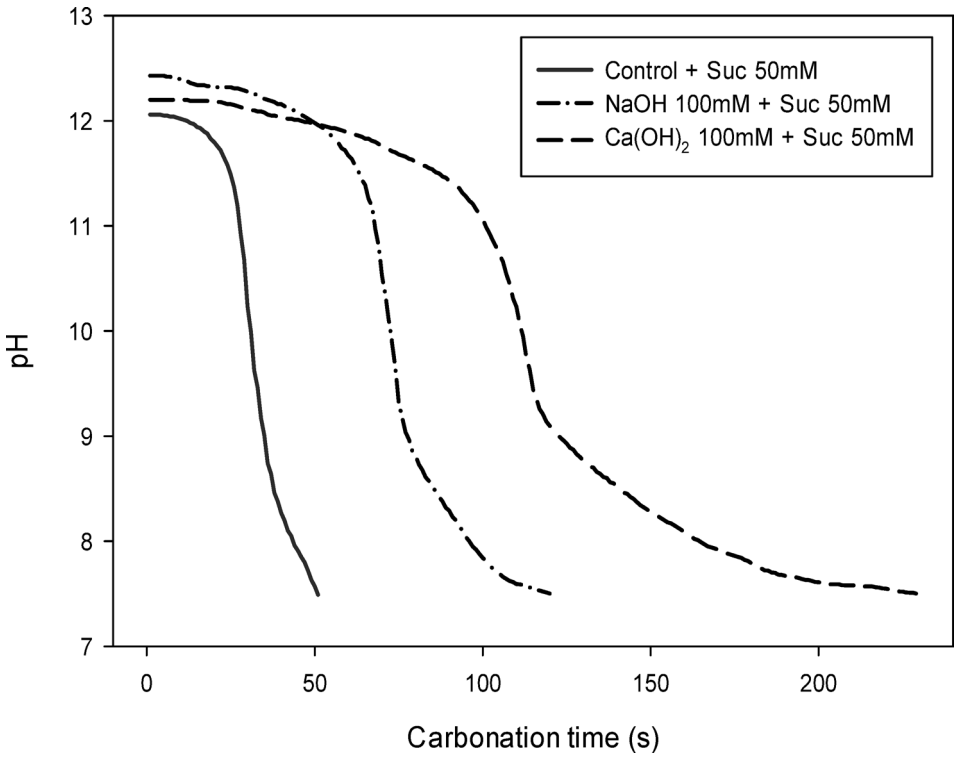

Fig. 2. Time-dependent pH changes during carbonation with various alkali additives.

The dissolution of CO_2, as outlined by Eqs. 5–8, leads to a reduction in the pH of the solution. The CO_3^{2-} ions produced during this reaction interact with Ca^{2+} ions in the eluate to produce $CaCO_3$ (Eq. 9).

In the carbonation process conducted in the absence of alkaline additives (control), the initial pH of the solution was high at 12.06 but rapidly decreased to 7.5 within approximately 50 s. Upon adding 100 mM $Ca(OH)_2$ with 50 mM sucrose to the calcium eluate, only a small amount of the $Ca(OH)_2$ initially dissolved, causing a slight increase in pH from 12.06 to 12.20. As carbonation progressed and the pH dropped, the remaining undissolved $Ca(OH)_2$ gradually dissolved, releasing OH^- ions, which slowed down the pH decrease (Eq. 10). The pH eventually stabilized at 7.5 after around 220 s.

$$Ca\,(OH)_2\,(s) \leftrightarrow Ca^{2+}\,(aq) + 2OH^-\,(aq) \tag{10}$$

When 100 mM of NaOH with 50 mM sucrose was added, the initial pH of the solution rose from 12.06 to 12.43. Precipitates identified as $Ca(OH)_2$ were formed due to the elevated pH, which led to the precipitation of Ca^{2+} ions from the eluate. The pH of the solution stabilized at 7.5, approximately 120 s after the initiation of carbonation.

From a stoichiometric perspective, $Ca(OH)_2$ generates twice the quantity of OH^- ions compared to NaOH. Therefore, when utilizing an equivalent concentration of 100 mM of an alkaline additive, the carbonation duration for $Ca(OH)_2$ is anticipated to be approximately twice that of NaOH. Owing to the limited solubility of $Ca(OH)_2$ in water, a significant portion remained as an undissolved solid upon its initial introduction to the eluate. However, in the presence of sucrose, $Ca(OH)_2$ gradually dissolved as carbonation advanced, culminating in the completion of the carbonation process. These results suggest that $Ca(OH)_2$, in conjunction with sucrose, effectively mitigates the pH reduction induced by CO_2 dissolution, akin to NaOH, thereby affirming its appropriateness as an alkaline agent for pH swing procedures.

Production yields of $CaCO_3$

As depicted in Fig. 3, the inclusion of alkaline agents significantly boosted the yield of $CaCO_3$ compared to their absence. The yield increased in proportion to the alkaline agent quantity. Among these agents, $Ca(OH)_2$ yielded the highest amount of $CaCO_3$, followed by NaOH and the control. Particularly, $Ca(OH)_2$ led to a notably higher yield than NaOH. For example, the addition of 100 mM $Ca(OH)_2$ resulted in a production of 292–318 kg/ton-CKD of $CaCO_3$, marking an approximately 22% increase over the yield of 240–315 kg/ton-CKD achieved with 200 mM NaOH.

The production yield of $CaCO_3$ may vary based on factors such as the Ca concentration in the solution, carbonation time, and pH. When $Ca(OH)_2$ combined with sucrose was used as the alkaline agent, its strong pH buffering capacity during the CO_2 dissolution reaction allowed for prolonged CO_2 injection without a rapid pH decrease (Fig. 2). Consequently, a sufficient number of CO_3^{2-} ions was produced, converting most Ca^{2+} ions into $CaCO_3$. These findings indicate that this method effectively circumvents the issue of reduced $CaCO_3$ yield due to the short carbonation duration in control experiments. Furthermore, the dissolution of $Ca(OH)_2$

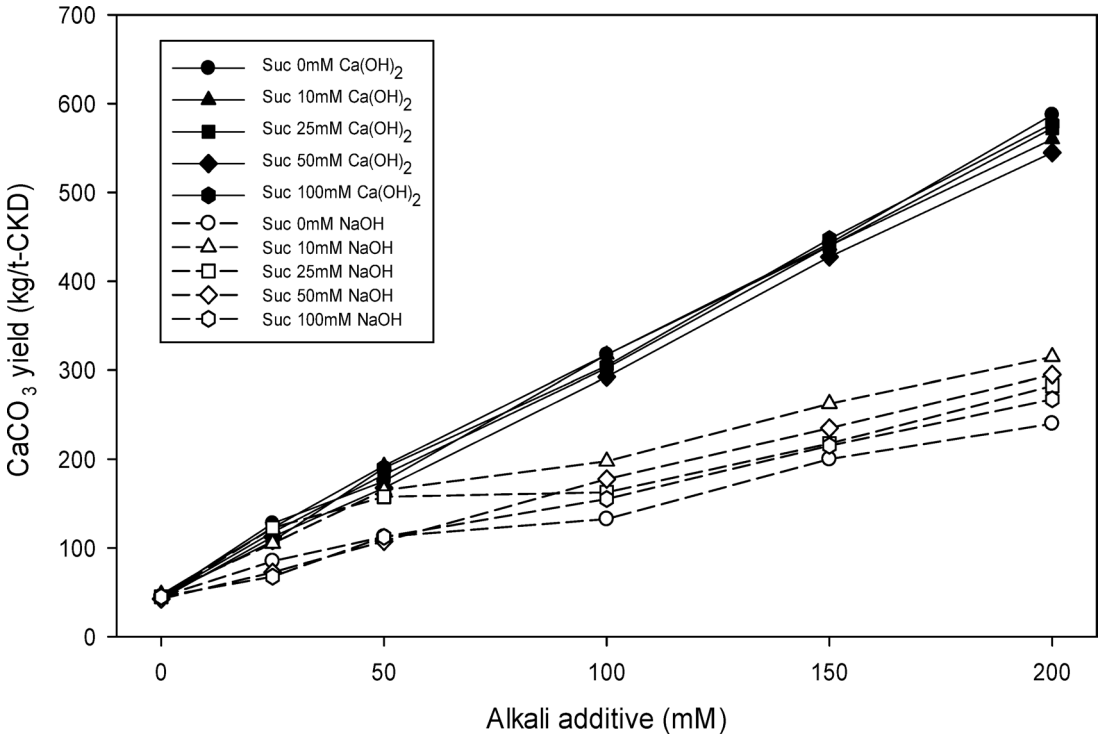

Fig. 3. Changes in $CaCO_3$ production yield with different amounts of alkali additives and sucrose.

introduced more Ca^{2+} ions into the solution, significantly enhancing the $CaCO_3$ production yield (Fig. 3). The inclusion of NaOH also increased the pH and provided a buffering effect, improving the conversion rate of Ca^{2+} ions into $CaCO_3$ and thereby increasing the production yield of $CaCO_3$. However, the yield is lower compared to that achieved with $Ca(OH)_2$, possibly due to the limited calcium content in the solution, which is restricted to the Ca^{2+} ions released before the carbonation process. Conversely, in the control experiment, the pH decreased sharply during carbonation, hindering sufficient CO_2 introduction and prematurely halting the carbonation reaction. Consequently, an insufficient amount of CO_3^{2-} ions is generated to fully convert the Ca^{2+} ions into $CaCO_3$, resulting in a low production yield of approximately 43–48 kg per ton of CKD.

In indirect carbonation, the production yield of $CaCO_3$ is a critical factor in assessing economic feasibility. As detailed in Section "Morphology of $CaCO_3$", it has been demonstrated that, in the presence of sucrose, the resulting $CaCO_3$ forms as vaterite, regardless of whether $Ca(OH)_2$ or NaOH is used as the alkali. To quantitatively compare the production yield of vaterite-type $CaCO_3$ based on different alkali additives, the costs of additives required to produce 1 ton of $CaCO_3$ were calculated using 100 mM of each alkali additive (Table 2). When $Ca(OH)_2$ was used, it was assumed that 10 mM sucrose would be added simultaneously. This selection of conditions was based on the following rationale: as shown in Table S3 and Fig. 6, the addition of 100 mM NaOH or 100 mM $Ca(OH)_2$ with 10 mM sucrose resulted in a comparable vaterite content (96%–99%) and particle size (2.0–2.1 µm).

As presented in Table 2, producing 1 ton of $CaCO_3$ costs $ 287 when using $Ca(OH)_2$ with sucrose, compared to $ 543 when using NaOH. The cost of using $Ca(OH)_2$, even when combined with sucrose, is approximately 53% of the cost of using NaOH. This cost difference is primarily due to the significantly lower price of $Ca(OH)_2$, which is only 32% of the price of NaOH. Although increasing sucrose concentrations beyond 10 mM improved vaterite content and reduced particle size, the associated rise in sucrose cost diminished the economic advantages of the $Ca(OH)_2$–sucrose system. As shown in Table 2, sucrose represents a major cost component, and at concentrations of 30 mM or higher, the total production cost approaches that of the conventional NaOH-based process. By comprehensively evaluating calcium carbonate yield, vaterite content (> 95%), spherical morphology, optimal particle size (~ 2 µm), and cost-effectiveness, the combination of 100 mM $Ca(OH)_2$ with 10 mM sucrose was identified as the most suitable balance. This combination offers a practical and economically viable approach for industrial-scale implementation of the $Ca(OH)_2$-based pH-swing carbonation process.

The cost of each additive was determined based on the latest market prices available online[29,30,39]. It is noteworthy that the cost estimation excluded the quantities and prices of CKD—an industrial by-product—and desalination brine—a by-product of seawater desalination. These materials must be removed or treated to mitigate environmental concerns, and their utilization is considered to offer potential economic benefits rather than being a cost burden.

In conclusion, utilizing $Ca(OH)_2$, even with the inclusion of sucrose, enables the generation of an equal quantity of $CaCO_3$ at approximately 53% of the expense in contrast to NaOH. This illustrates the significantly higher cost efficiency of $Ca(OH)_2$ over NaOH concerning the efficiency of vaterite-type $CaCO_3$ production.

Morphology of $CaCO_3$

Figure 4 illustrates the vaterite content variations of $CaCO_3$ generated with different alkali additives and sucrose concentrations. Without sucrose, NaOH as the alkali agent resulted in the predominant formation of vaterite crystals, whereas $Ca(OH)_2$ led to calcite formation. The vaterite content varied notably, ranging from 89.1% to 99% with NaOH and from 3.7% to 49.1% with $Ca(OH)_2$. Conversely, combining $Ca(OH)_2$ with sucrose significantly increased the vaterite content to approximately 99% (Fig. 4 and Table S3).

This section examines the factors that lead to the high vaterite content obtained when $Ca(OH)_2$ is employed as the alkaline agent along with sucrose. It is widely recognized that a high degree of supersaturation and a rapid nucleation rate of $CaCO_3$ are favorable conditions for vaterite formation[40,41].

$$S = \left(\frac{\alpha_{Ca^{2+}} \cdot \alpha_{CO_3^{2-}}}{K_{sp}} \right)^{1/2} \tag{11}$$

Here, S represents the supersaturation, while $\alpha_{Ca^{2+}}$ and $\alpha_{CO_3^{2-}}$ denote the activities of calcium and carbonate ions, respectively. When $Ca(OH)_2$ is utilized as an alkaline additive, $CaCO_3$ can be produced through two primary reaction pathways during the carbonation process.

$$Ca(OH)_2\,(s) + CO_3^{2-}\,(aq) \rightarrow CaCO_3\,(s) + 2OH^- \tag{12}$$

$$Ca^{2+}\,(aq) + CO_3^{2-}\,(aq) \rightarrow CaCO_3\,(s) \tag{13}$$

Additive (mM)			Cost ($)			
$Ca(OH)_2$	Sucrose	NaOH	$Ca(OH)_2$*	Sucrose**	NaOH***	Total cost ($)
100	10		132.3	155.1		287.4
		100			542.6	542.6

Table 2. Comparison of production costs for 1 ton of $CaCO_3$ using two different alkaline additives. *$Ca(OH)_2$: $ 227.0/ton[29], **Sucrose: $ 575.5/ton[39], ***NaOH: $ 719.0/ton[30].

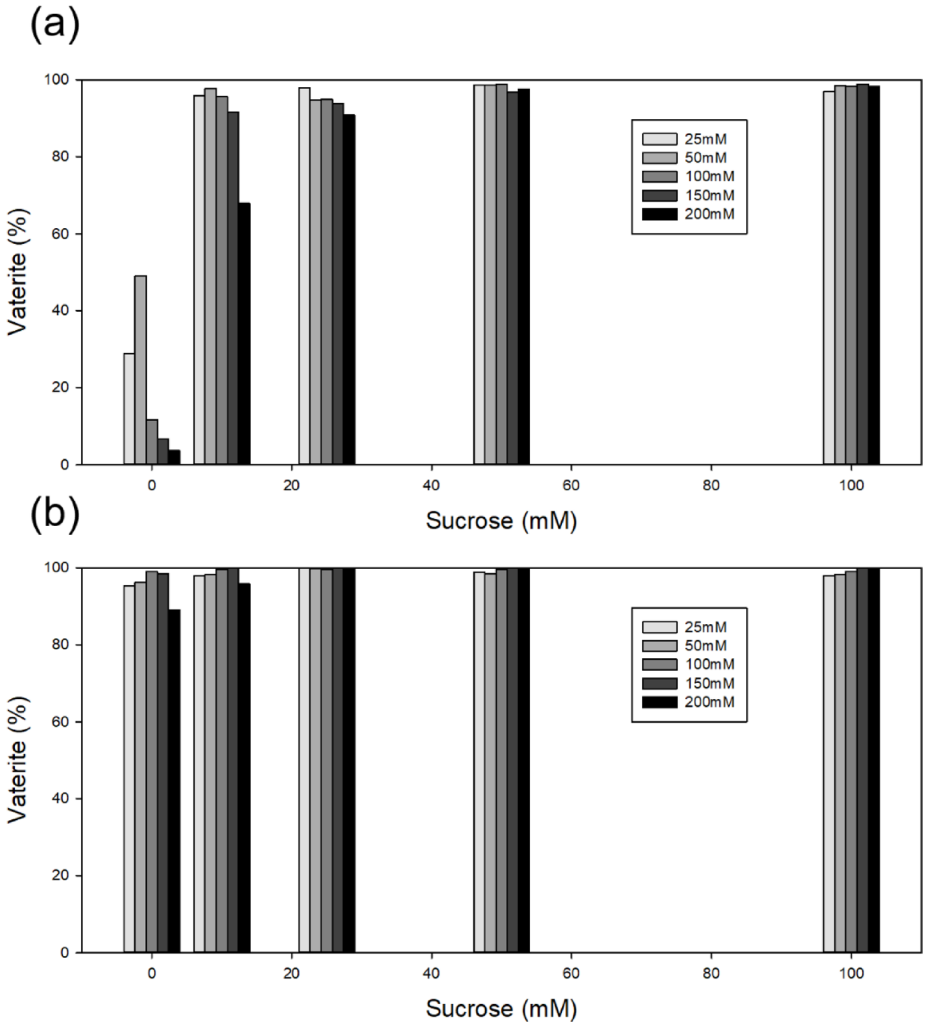

Fig. 4. Changes in the vaterite content of $CaCO_3$ produced with different alkali additives and sucrose concentrations: (**a**) $Ca(OH)_2$, (**b**) NaOH.

The first pathway involves the reaction between solid-state $Ca(OH)_2$ and CO_3^{2-} ions, while the second pathway occurs through ionic bonding between Ca^{2+} ions and CO_3^{2-} ions in the solution [15,24]. In the first pathway, the reaction is localized, as CO_3^{2-} ions adsorb onto the surface of $Ca(OH)_2$, resulting in a slower reaction rate due to the solid–ion interaction [38,41]. Consequently, the nucleation rate is relatively slow. In contrast, the second pathway occurs uniformly throughout the solution, with the ionic bonding reaction proceeding significantly faster than the first pathway, leading to a much higher nucleation rate. Therefore, the second reaction pathway is favorable for vaterite formation.

As previously mentioned, $Ca(OH)_2$ exhibits very low solubility in water. In the present study, brine was used as a solvent. The eluate had a high initial pH exceeding 12, leading to the minimal dissolution of $Ca(OH)_2$ upon its addition to the solution, thereby retaining most of the $Ca(OH)_2$ in its solid state. Consequently, the inclusion of $Ca(OH)_2$ did not significantly affect the supersaturation of the solution. Upon the introduction of CO_2 into this suspension, $CaCO_3$ is formed because of a reaction with the undissolved $Ca(OH)_2$ (Eq. 12), hindering vaterite formation. This elucidates the limited vaterite content (3.7%–49.1%) in the $CaCO_3$ produced by solely adding $Ca(OH)_2$, without sucrose, to the calcium eluate, as shown in Fig. 4 and Table S3.

To address the challenges related to low supersaturation and slow nucleation rates when utilizing $Ca(OH)_2$ as an alkaline agent, carbonation experiments were conducted with the inclusion of sucrose. Sucrose boosts the dissolution of $Ca(OH)_2$ and aids in the absorption of gaseous CO_2 into the solution, thereby elevating the supersaturation level[32,42]. Previous studies by our group have confirmed the beneficial impact of sucrose on promoting vaterite formation[23]. Upon simultaneous addition of $Ca(OH)_2$ and sucrose to the calcium eluate, the analysis of calcium concentration before carbonation indicated that higher levels of Ca^{2+} ions and increased supersaturation were achieved with escalating sucrose concentrations (Fig. S1). For example, the introduction of 100 mM sucrose increased the Ca^{2+} ion concentration from 5415 mg/L to 7100 mg/L. Consequently, the outcomes of the carbonation experiments exhibited a noticeable trend of augmented vaterite content. Specifically, with the addition of just 10 mM sucrose to 200 mM $Ca(OH)_2$, the vaterite content notably increased from 3.7% to 67.9%, further escalating to 98.3% with 100 mM sucrose (Fig. 4 and Table S3).

When NaOH was utilized as the alkaline additive, it readily dissociated in the eluate, unlike $Ca(OH)_2$, rapidly and significantly increasing the pH of the solution. This rapid increase in the pH accelerated CO_2 absorption, and the resulting increase in $\alpha_{CO^{2-}_3}$ enhanced the supersaturation level, creating favorable conditions for vaterite formation[43]. Consequently, vaterite was the primary crystal form of $CaCO_3$ produced through the carbonation process, with a content exceeding 95%, even in the absence of sucrose. However, the addition of an excessive amount of NaOH (approximately 200 mM) caused an excessive increase in the solution's pH, resulting in the precipitation of some Ca^{2+} ions as $Ca(OH)_2$. This led to a decrease in $\alpha_{Ca^{2+}}$, thereby reducing the supersaturation level. Additionally, the interaction between the precipitated $Ca(OH)_2$ and CO_3^{2-} ions slowed the nucleation rate, leading to a vaterite content of approximately 89% (Fig. 4 and Table S3). Nevertheless, when NaOH was combined with sucrose, similar to the experiments with $Ca(OH)_2$, the vaterite content increased to 100% (Fig. 4 and Table S3).

Figure 5 displays the SEM results of $CaCO_3$ synthesized using $Ca(OH)_2$ and NaOH as alkaline agents. The utilization of $Ca(OH)_2$ in the absence of sucrose resulted in the formation of cubic calcite (Fig. 5a), whereas NaOH yielded spherical vaterite (Fig. 5e). When sucrose was present, the spherical structure and porosity of vaterite formed with $Ca(OH)_2$ and NaOH exhibited no significant differences (Fig. 5b–d and f–h).

$CaCO_3$ particle size and purity

As depicted in Figs. 6 and S2, the particle sizes (D_{50}) of $CaCO_3$ produced using $Ca(OH)_2$ and NaOH as alkaline agents were similar, ranging from 0.7 to 2.5 μm and 0.6 to 2.4 μm, respectively. Moreover, with the same sucrose concentration, minimal variation in the particle size distribution was observed between the use of $Ca(OH)_2$ and NaOH (Fig. S3). Increasing the sucrose amount up to 50 mM led to a decrease in $CaCO_3$ particle size. However, at a sucrose concentration of 100 mM, the particle size either increased or remained stable. This behavior is attributed to the residual sucrose, which, not binding to calcium, enhances the viscosity of the solution, thereby facilitating the aggregation of $CaCO_3$ particles[23].

When the sucrose concentration was 25 mM or lower, the particle size of $CaCO_3$ produced using $Ca(OH)_2$ was larger than that produced using NaOH. However, when the sucrose concentration exceeded 50 mM, no significant difference in particle size was observed between the two methods. This outcome is attributed to the increased supersaturation, nucleation rate, and number of nuclei resulting from the addition of sucrose[23]. In the absence of sucrose, the larger particle size of $CaCO_3$ is a consequence of the higher calcite content. It is widely recognized that calcite-type $CaCO_3$ typically exhibits larger particle sizes compared to vaterite-type $CaCO_3$[23,44].

The purity of $CaCO_3$ significantly affects its applications and market value. $CaCO_3$ produced using $Ca(OH)_2$ exhibited a purity range of 96%–98%, while that produced using NaOH had a purity range of 97%–98%. The overall purity of $CaCO_3$ remained consistently high, showing no significant differences based on the type of alkaline additives used, even when using brine as a solvent. The XRF and XRD analyses revealed that sulfur, primarily in the form of gypsum ($CaSO_4$), was the main impurity (Table S4 and Fig. S3). This impurity formation is attributed to the high concentration of SO_4^{2-} ions in the brine and the increased Ca^{2+} ion concentration during the elution process, leading to the supersaturation of $CaSO_4$ and subsequent precipitation[45]. $CaSO_4$ is concentrated and precipitated during the RO desalination process owing to the presence of Ca^{2+} and SO_4^{2-} ions in seawater. It can also precipitate locally under supersaturated conditions resulting from seawater evaporation[46]. Furthermore, $CaSO_4$ is a naturally occurring stable compound commonly found in the environment, remaining inert under various climatic and chemical conditions without releasing toxic substances[47].

As shown in Table 1, although the Fe content in CKD is relatively high at 2.88 wt.%, that in the produced $CaCO_3$ was determined to be 0. This observation indicates that Fe did not dissolve in the brine, suggesting the

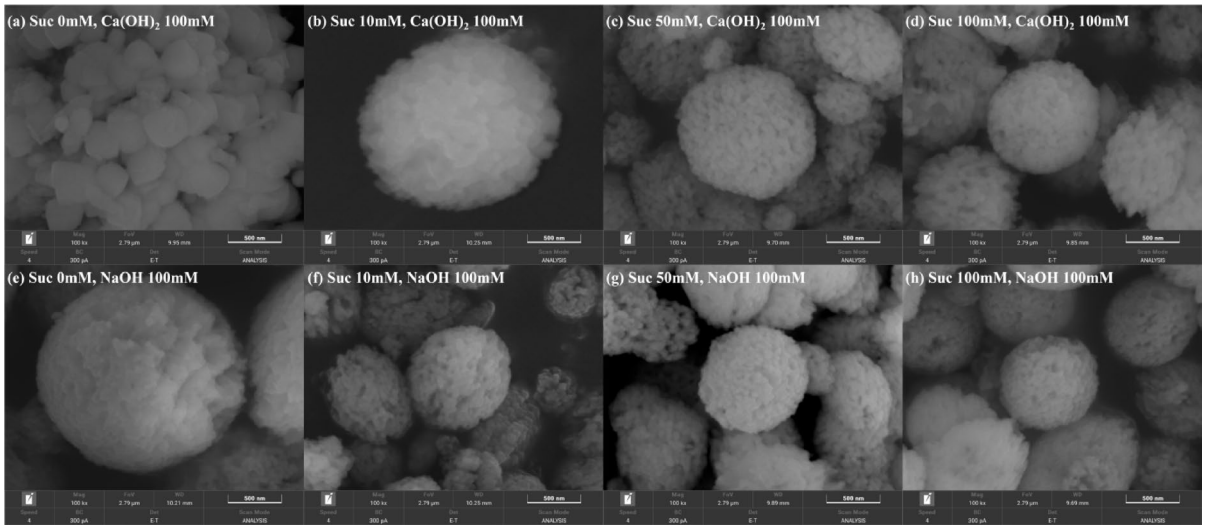

Fig. 5. SEM images of produced $CaCO_3$ using $Ca(OH)_2$ and NaOH with sucrose concentrations at (**a**, **e**) 0 mM, (**b**, **f**) 10 mM, (**c**, g) 50 mM, and (**d**, **h**) 100 mM.

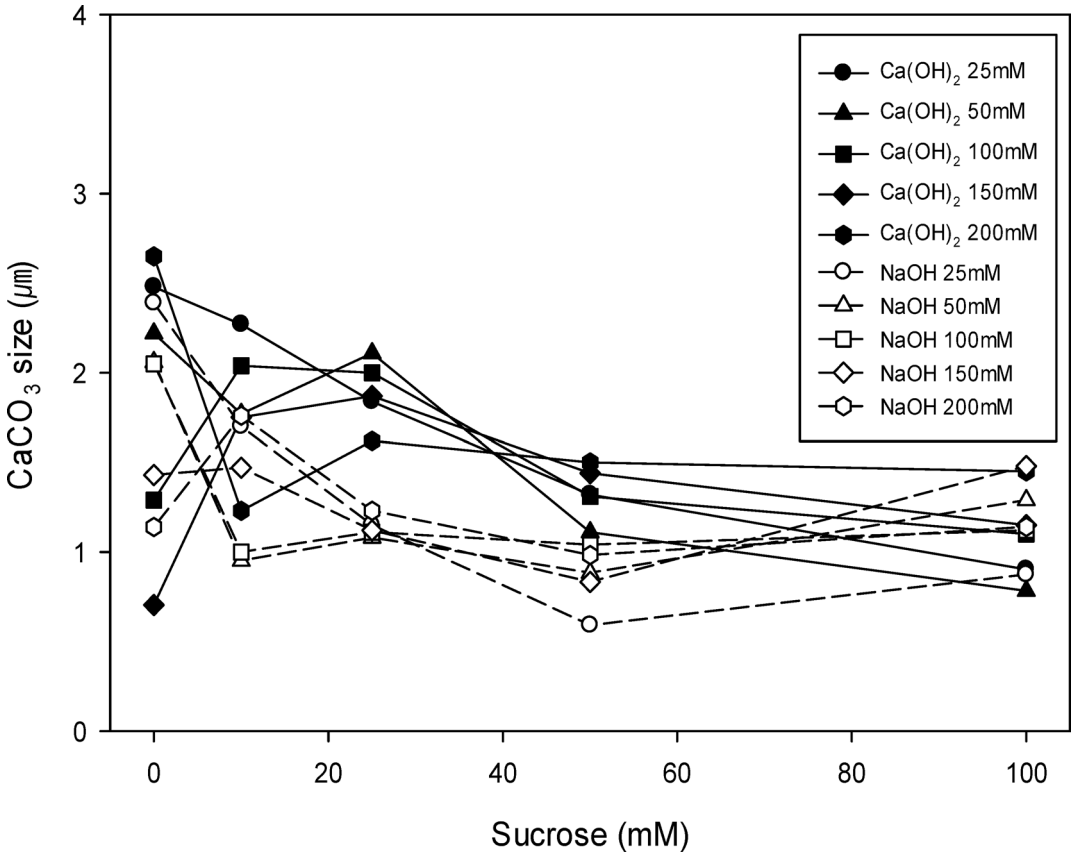

Fig. 6. Comparison of changes in $CaCO_3$ particle size with varying sucrose concentrations using $Ca(OH)_2$ and NaOH as alkali agents.

potential to simplify the pH-swing process to a single carbonation step. This could eliminate the need for an additional stage to remove impurities such as Fe[48]. The $CaCO_3$ produced through this method contains minimal impurities, with negligible effects on its performance in various industrial applications. Therefore, the resulting $CaCO_3$ can be utilized in diverse industries, including paper manufacturing, paints and coatings, as well as environmental and agricultural sectors[22].

Conclusions

This study investigated the feasibility of using $Ca(OH)_2$ as a cost-effective and safer alternative to NaOH in the pH swing process for producing vaterite-type $CaCO_3$ via indirect carbonation, using desalination brine as a solvent. Despite its low solubility, $Ca(OH)_2$, when combined with sucrose, effectively buffered the pH during carbonation, significantly enhancing the yield of vaterite-type $CaCO_3$ compared to that achieved by using NaOH. The $CaCO_3$ obtained with $Ca(OH)_2$ had a high purity of 96–98% and controlled particle size, similar to that achieved with NaOH, indicating its suitability for meeting industrial standards for high-purity vaterite production. Cost analysis revealed that substituting NaOH with $Ca(OH)_2$ decreased the overall production cost of $CaCO_3$ by approximately 53%, highlighting its economic viability. The inclusion of sucrose was crucial for enhancing the dissolution of $Ca(OH)_2$, increasing supersaturation, and creating favorable conditions for vaterite formation.

This study demonstrates that $Ca(OH)_2$, particularly when combined with sucrose, is a viable and efficient alternative to NaOH in the pH-swing process. It offers significant economic, safety, and environmental benefits while facilitating the production of high-purity, vaterite-type $CaCO_3$. These findings support the potential for broader industrial applications of $Ca(OH)_2$ in carbonation processes and contribute to the development of cost-effective and sustainable CCUS technologies. Furthermore, these results underscore the alignment of this approach with the principles of sustainable development and cleaner production by utilizing industrial byproducts and minimizing chemical inputs. Nonetheless, further studies are needed to address potential scale-up challenges, such as mixing efficiency, reaction time, and solid–liquid separation under actual industrial conditions. Future research should focus on optimizing process parameters to maximize vaterite yield, reduce costs, and improve overall efficiency. Additionally, pilot- and industrial-scale experiments are essential to evaluate the scalability and operational feasibility of utilizing $Ca(OH)_2$ in large-scale pH-swing processes.

Data availability

Data is provided within the manuscript or supplementary information files.

Received: 20 February 2025; Accepted: 12 May 2025
Published online: 19 May 2025

References

1. NOAA, National Oceanic and Atmospheric Administration. During a year of extremes, carbon dioxide levels surge faster than ever. https://www.noaa.gov/news-release/during-year-of-extremes-carbon-dioxide-levels-surge-faster-than-ever (2024).
2. C3S, Copernicus Climate Change Service. Greenhouse gas concentrations. https://climate.copernicus.eu/esotc/2023/greenhouse-gas-concentrations (2024).
3. Iida, Y., Takatani, Y., Kojima, A. & Ishii, M. Global trends of ocean CO2 sink and ocean acidification: An observation-based reconstruction of surface ocean inorganic carbon variables. *J. Oceanogr.* **77**, 323–358 (2021).
4. Fontela, M., Velo, A., Gilcoto, M. & Pérez, F. F. Anthropogenic CO_2 and ocean acidification in Argentine Basin Water Masses over almost five decades of observations. *Sci. Total Environ.* **779**, 146570 (2021).
5. Gao, K., Zhang, Y. & Häder, D. P. Individual and interactive effects of ocean acidification, global warming, and UV radiation on phytoplankton. *J. Appl. Phycol.* **30**, 743–759. https://doi.org/10.1007/s10811-017-1329-6 (2018).
6. He, M. et al. Simultaneous CO_2 mineral sequestration and rutile beneficiation by using titanium-bearing blast furnace slag: Process description and optimization. *Energy* **248**, 123643 (2022).
7. Sim, G. et al. Simultaneous CO_2 utilization and rare earth elements recovery by novel aqueous carbon mineralization of blast furnace slag. *J. Environ. Chem. Eng.* **10**, 107327 (2022).
8. Ren, E. et al. Carbon dioxide mineralization for the disposition of blast-furnace slag: Reaction intensification using NaCl solutions. *Greenh. Gases Sci. Technol.* **10**, 436–448 (2020).
9. Yi, Y. R. et al. Accelerated carbonation of ladle furnace slag and characterization of its mineral phase. *Constr. Build. Mater.* **276**, 122235 (2021).
10. Tong, Z., Ma, G., Zhou, D., Yang, G. & Peng, C. The indirect mineral carbonation of electric arc furnace slag under microwave irradiation. *Sci. Rep.* **9**, 7676 (2019).
11. Liu, X. et al. Glycine-induced synthesis of vaterite by direct aqueous mineral carbonation of desulfurization gypsum. *Environ. Chem. Lett.* **20**, 2261–2269 (2022).
12. Ding, W., Chen, Q., Sun, H. & Peng, T. Modified mineral carbonation of phosphogypsum for CO_2 sequestration. *J. CO2 Util.* **34**, 507–515 (2019).
13. Azdarpour, A. et al. CO_2 sequestration using red gypsum via pH-swing process: Effect of carbonation temperature and NH_4HCO_3 on the process efficiency. *Int. J. Miner. Process.* **169**, 27–34 (2017).
14. Irfan, M. F. et al. Modeling and optimization of aqueous mineral carbonation for cement kiln dust using response surface methodology integrated with Box-Behnken and central composite design approaches. *Min. Metall. Explor.* **37**, 1367–1383 (2020).
15. Jeon, J. & Kim, M. J. CO_2 storage and $CaCO_3$ production using seawater and an alkali industrial by-product. *Chem. Eng. J.* **378**, 122180 (2019).
16. Puthanveettil, R. K., Kim, S. & Kim, M. J. Utilizing seawater and brine to simultaneously produce high-purity magnesium sulfate and vaterite-type calcium carbonate. *Desalination* **578**, 117436 (2024).
17. Bang, J. H. et al. Sequential carbonate mineralization of desalination brine for CO_2 emission reduction. *J. CO2 Util.* **33**, 427–433 (2019).
18. Altiner, M. Effect of base types on the properties of MgO particles obtained from dolomite ore. *Min. Eng.* **71**, 56–57 (2019).
19. Xia, M., Ye, C., Pi, K., Liu, D. & Gerson, A. R. Ca removal and Mg recovery from flue gas desulfurization (FGD) wastewater by selective precipitation. *Water Sci. Technol.* **76**, 2842–2850 (2017).
20. Kim, I. et al. Two-step mineral carbonation using seawater-based industrial wastewater: An eco-friendly carbon capture, utilization, and storage process. *J. Mater. Cycles Waste Manag.* **22**, 333–347 (2020).
21. Azdarpour, A. et al. A review on carbon dioxide mineral carbonation through pH-swing process. *Chem. Eng. J.* **279**, 615–630. https://doi.org/10.1016/j.cej.2015.05.064 (2015).
22. Fadia, P. et al. Calcium carbonate nano- and microparticles: synthesis methods and biological applications. *3 Biotech* **11**, 1–30. https://doi.org/10.1007/s13205-021-02995-2 (2021).
23. Kim, G., Kim, S. & Kim, M. J. Effect of sucrose on CO_2 storage, vaterite content, and $CaCO_3$ particle size in indirect carbonation using seawater. *J. CO2 Util.* **57**, 101894 (2022).
24. Kim, S., Jeon, J. & Kim, M. J. Vaterite production and particle size and shape control using seawater as an indirect carbonation solvent. *J. Environ. Chem. Eng.* **10**, 107296 (2022).
25. Remya, K. P., Kim, S. & Kim, M. J. Surfactant-free hydrothermal fabrication of vaterite $CaCO_3$ with hexagonal bipyramidal morphologies using seawater. *Powder Technol.* **410**, 117865 (2022).
26. Kim, S., Koh, E. & Kim, M. J. Recovery of high-purity hydromagnesite from seawater through carbonation using $Ca(OH)_2$. *Desalination* **586**, 117907 (2024).
27. Sarkhel, R., Sahu, C., Kumar, R. & Sangwai, J. S. Effects of sodium hydroxide and calcium hydroxide on the phase equilibria of methane hydrates. *J. Chem. Thermodyn.* **177**, 106935 (2023).
28. Cai, G.-X. Ammonia volatilization. In *Nitrogen in Soils of China* 193–213 (Springer, 1997).
29. Made-in-China. Bulk Calcium Hydroxide Factory Price $Ca(OH)_2$ MSDS Calcium Hydroxide for Sale. https://hongyu8888.en.made-in-china.com/product/XmPpQKalYjVW/China-Bulk-Calcium-Hydroxide-Factory-Price-Ca-oh-2-MSDS-Calcium-Hydroxide-for-Sale.html. Accessed 17 Jan 2025.
30. Made-in-China. Caustic Soda Pearls Factory Supply NaOH CAS 1310-73-2 Sodium Hydroxide Good Price. https://zhonghongda.en.made-in-china.com/product/odqTKelynYGE/China-Caustic-Soda-Pearls-Factory-Supply-Naoh-CAS-1310-73-2-Sodium-Hydroxide-Good-Price.html. Accessed 17 Jan 2025.
31. Jiang, D. et al. Comparison of sodium hydroxide and calcium hydroxide pretreatments of giant reed for enhanced enzymatic digestibility and methane production. *Bioresour. Technol.* **244**, 1150–1157 (2017).
32. O'Neil, M. J. *The Merck Index* 15th edn. (Royal Society of Chemistry, 2013).
33. Kester, D. R., Duedall, I. W., Connors, D. N. & Pytkowicz, R. M. Preparation of artificial seawater. *Limnol. Oceanogr.* **12**, 176–179. https://doi.org/10.4319/lo.1967.12.1.0176 (1967).
34. Rao, M. S. Kinetics and mechanism of the transformation of vaterite to calcite. *Bull. Chem. Soc. Jpn.* **46**, 1414–1417 (1973).
35. Cho, T. & Kim, M. J. Synthesis of magnesium sulfate from seawater using alkaline industrial wastes, sulfuric acid, and organic solvents. *Sep. Sci. Technol.* **54**, 2749–2757 (2019).
36. Na, H. R. & Kim, M. J. Determination of optimal conditions for magnesium recovery process from seawater desalination brine using paper sludge ash, sulfuric acid, and ethanol. *Desalin. Water Treat.* **157**, 324–331 (2019).
37. Jo, H., Jang, Y. N. & Young Jo, H. Influence of NaCl on mineral carbonation of CO_2 using cement material in aqueous solutions. *Chem. Eng. Sci.* **80**, 232–241 (2012).
38. Han, S. J., Yoo, M., Kim, D. W. & Wee, J. H. Carbon dioxide capture using calcium hydroxide aqueous solution as the absorbent. *Energy Fuels* **25**, 3825–3834 (2011).
39. ICE. Intercontinental Exchange. White Sugar Futures Data. https://www.ice.com/products/37089080/White-Sugar-Futures/data?marketId=7303333&span=2 (2025)

40. Oral, Ç. M. & Ercan, B. Influence of pH on morphology, size and polymorph of room temperature synthesized calcium carbonate particles. *Powder Technol.* **339**, 781–788 (2018).
41. Kim, J. S. & Jo, H. Y. Formation of calcium carbonates from $Ca(OH)_2$-H_2O-supercritical CO_2 using a rapid spraying method. *Korean J. Chem. Eng.* **37**, 1086–1096 (2020).
42. Konopacka-Łyskawa, D., Czaplicka, N., Kościelska, B., Łapiński, M. & Gębicki, J. Influence of selected saccharides on the precipitation of calcium-vaterite mixtures by the CO_2 bubbling method. *Crystals* **9**, 117 (2019).
43. Putta, K. R., Pinto, D. D. D., Svendsen, H. F. & Knuutila, H. K. CO_2 absorption into loaded aqueous MEA solutions: Kinetics assessment using penetration theory. *Int. J. Greenh. Gas Control* **53**, 338–353 (2016).
44. Ševčík, R., Šašek, P. & Viani, A. Physical and nanomechanical properties of the synthetic anhydrous crystalline $CaCO_3$ polymorphs: Vaterite, aragonite and calcite. *J. Mater. Sci.* **53**, 4022–4033 (2018).
45. Reiss, A. G. et al. Gypsum precipitation under saline conditions: Thermodynamics, kinetics, morphology, and size distribution. *Minerals* **11**, 141. https://doi.org/10.3390/min11020141 (2021).
46. Ziegenheim, S., Peintler, G., Pálinkó, I. & Sipos, P. The kinetics of the precipitation of gypsum, $CaSO_4 \cdot 2H_2O$, over a wide range of reactant concentrations. *React. Kinet. Mech. Catal.* **131**, 75–88 (2020).
47. Freyer, D. & Voigt, W. Crystallization and phase stability of Ca_SO_4 and $CaSO_4$—based salts. *Monatsh. Chem.* **134**, 693–719. https://doi.org/10.1007/s00706-003-0590-3 (2003).
48. Wang, B., Pan, Z., Cheng, H., Zhang, Z. & Cheng, F. A review of carbon dioxide sequestration by mineral carbonation of industrial byproduct gypsum. *J. Clean. Prod.* **302**, 126930. https://doi.org/10.1016/j.jclepro.2021.126930 (2021).

Acknowledgements

This work was supported by the National Research Foundation (NRF) of Korea grant funded by the Korean government (RS-2024-00337666).

Author contributions

W.J.: Data curation, Investigation, Methodology, Validation, Visualization, Writing—original draft, M.K.: Conceptualization, Funding acquisition, Supervision, Writing-review & editing. All authors reviewed the manuscript.

Declarations

Competing interests

The authors declare no competing interests.

Additional information

Supplementary Information The online version contains supplementary material available at https://doi.org/10.1038/s41598-025-02118-4.

Correspondence and requests for materials should be addressed to M.-J.K.